Science Advances

AAAS

advances.sciencemag.org/cgi/content/full/4/6/eaat1687/DC1

Supplementary Materials for

A pyrolyzed polyacrylonitrile/selenium disulfide composite cathode with remarkable lithium and sodium storage performances

Zhen Li, Jintao Zhang, Yan Lu, Xiong Wen (David) Lou

Published 8 June 2018, *Sci. Adv.* **4**, eaat1687 (2018)
DOI: 10.1126/sciadv.aat1687

This PDF file includes:

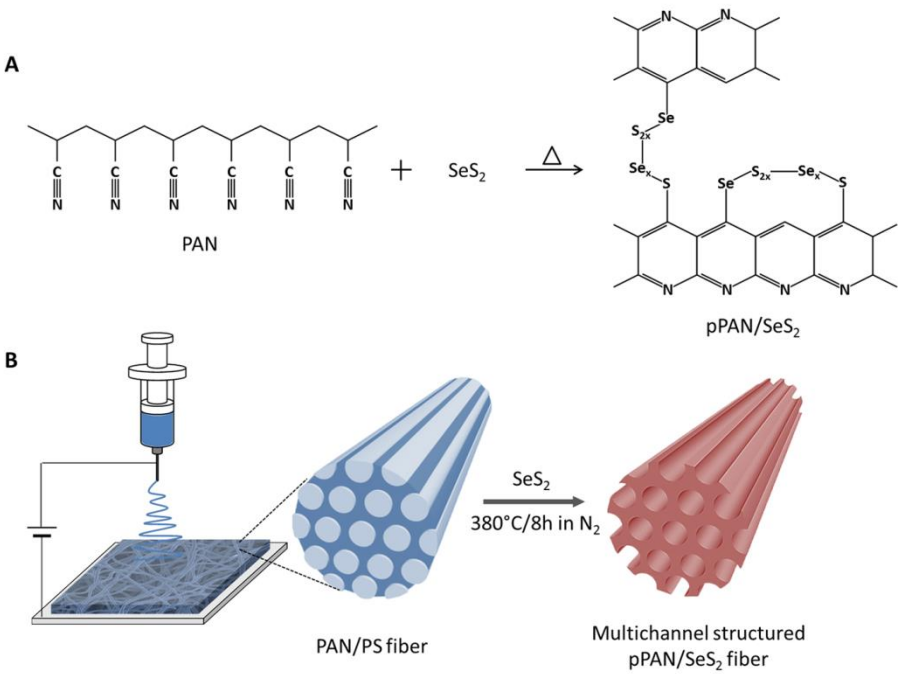

fig. S1. Schematic illustrations of the chemical structure and synthesis method. (**A**) The proposed chemical structure of pPAN/SeS_2. (**B**) The synthesis process of pPAN/SeS_2.

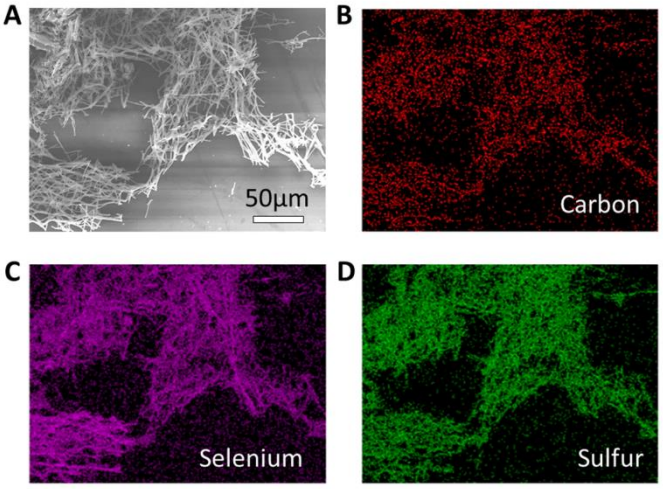

fig. S2. EDX mappings of pPAN/SeS_2. (**A**) SEM image of pPAN/SeS_2 and the corresponding elemental distributions of (**B**) C, (**C**) Se and (**D**) S.

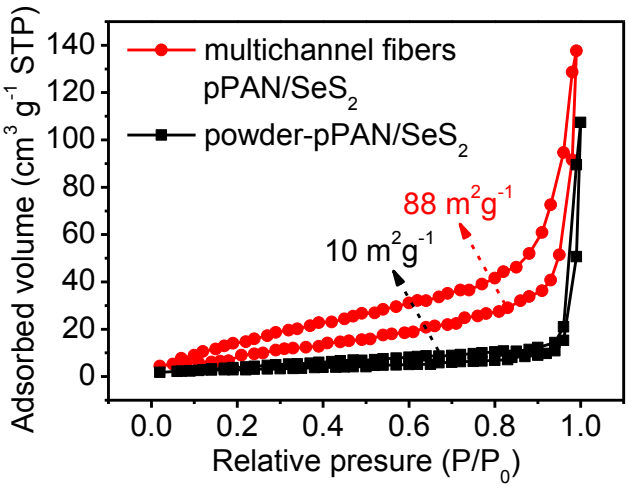

fig. S3. N_2 sorption isotherms of multichannel pPAN/SeS_2 fibers and pPAN/SeS_2 powder. Due to the decomposing of PS at elevated temperature, the multichannel pPAN/SeS_2 fibers show a BET specific surface area of 88 m^2 g^{-1} which is nearly 8 times higher than that of the pPAN/SeS_2 powder (10 m^2 g^{-1}).

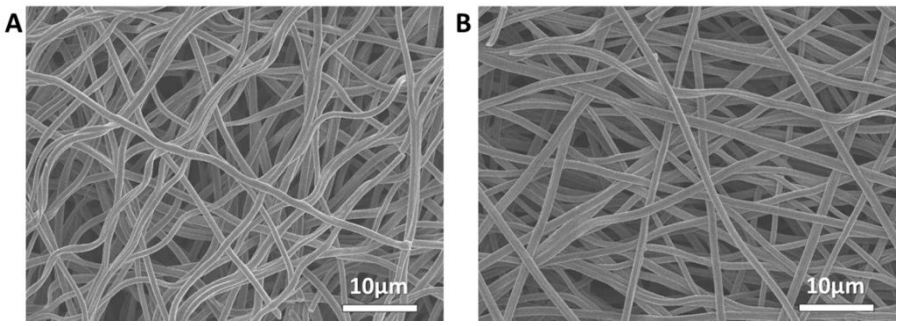

fig. S4. Morphology characterizations. SEM images of (**A**) pPAN/S and (**B**) pPAN/Se.

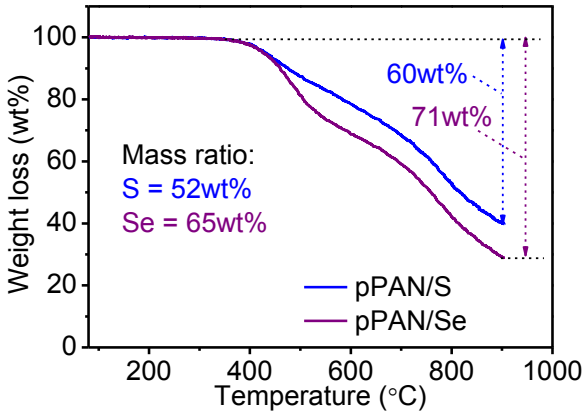

fig. S5. TGA curves of pPAN/S and pPAN/Se. Based on that pure pPAN losses 17 wt% of weight when heated to 900 °C in N_2 atmosphere, the mass ratios of S and Se in pPAN/S and pPAN/Se are calculated to be 52 wt% and 65 wt%, respectively.

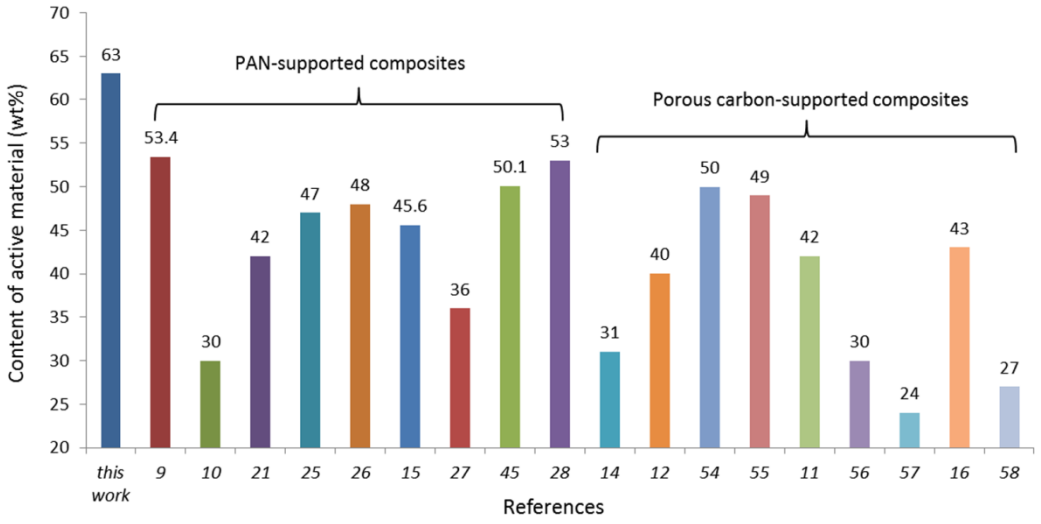

fig. S6. The active material contents of various PAN-supported or microporous carbon-supported composites for Li-S or Li-Se/S batteries. The composite cathodes for comparison are selected from recent studies, in which the cathodes are well matched with $LiPF_6$-carbonate-based electrolytes: pPAN/S(*9*), pPAN/S(*10*), SPAN(*21*), pPAN-S/GNS(*25*), pPAN-S/MWCNT(*26*), SPAN4(*15*), PAN-S-VA(*27*), Se/PAN(*45*), C/S/PAN(*28*), C/S(*14*), S/(CNT@MPC)(*12*), $S_{0.94}Se_{0.06}$/C(*54*), $S_{0.94}Se_{0.06}$@PCNFs(*55*), C/S(*11*), C/S(*56*), NC/S(*57*), MCP/S(*16*), and S/CA(*58*).

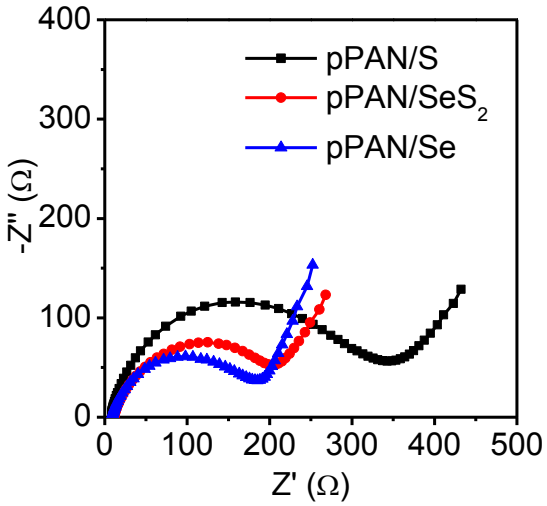

fig. S7. EIS of pPAN/S, pPAN/SeS_2, and pPAN/Se. The Nyquist plots of different groups were collected from 100 kHz to 1Hz before cycling tests.

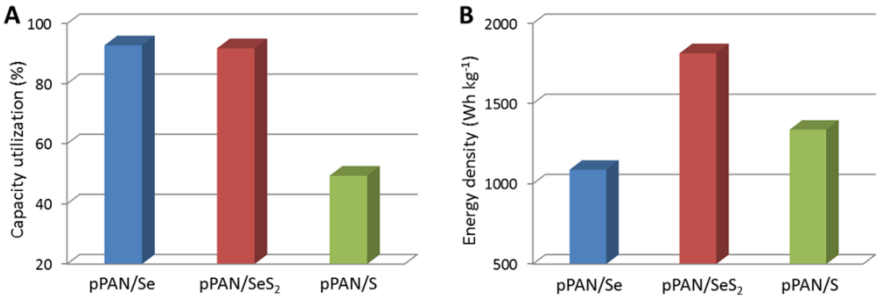

fig. S8. Comparisons of capacity utilization and energy density for Li storage. Comparisons on (**A**) capacity utilization and (**B**) energy density of pPAN/S, pPAN/SeS_2, and pPAN/Se for Li-storage at 0.5 A g^{-1}. The capacity utilizations are calculated based on the specific capacities and theoretical capacities of S, SeS_2 and Se, respectively. The voltage values used for calculating energy densities are selected at 50 % depth of discharge (DOD).

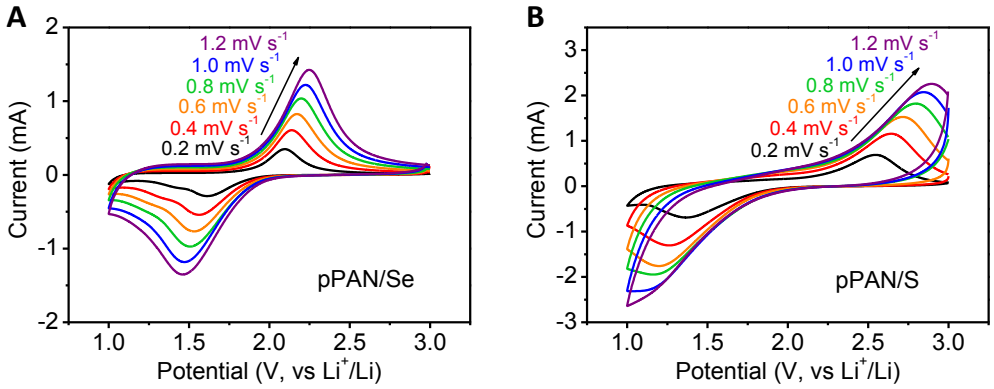

fig. S9. CV curves from 0.2 to 1.2 mV s^{-1}. CV curves of (**A**) pPAN/Se and (**B**) pPAN/S in voltage range of 1.0 – 3.0 V with Li metal as anode.

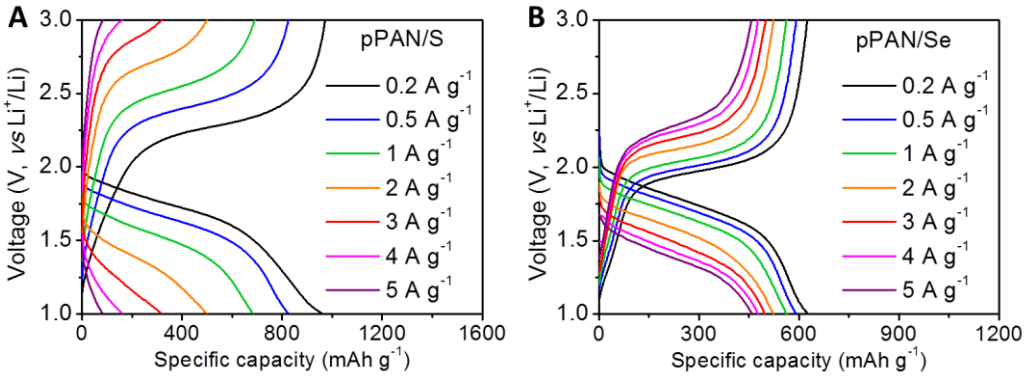

fig. S10. Rate performances. Voltage profiles of (**A**) pPAN/S and (**B**) pPAN/Se at various current densities from 0.2 to 5 A g^{-1} for Li storage.

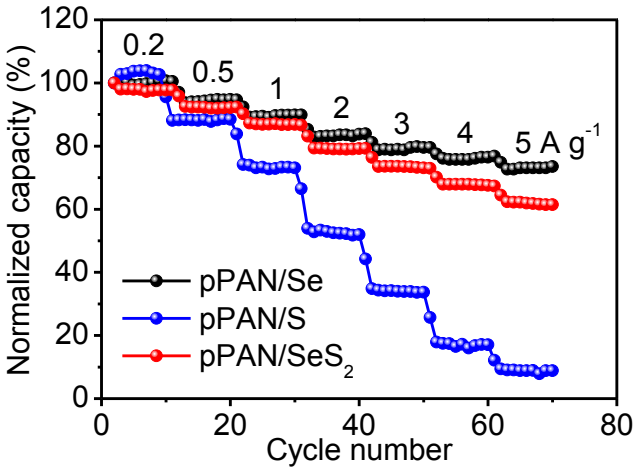

fig. S11. Comparison of normalized capacities. Normalized capacities at various current densities from 0.2 to 5 A g^{-1} of pPAN/S, pPAN/SeS_2, and pPAN/Se for Li-storage. The normalized capacity is based on the 2nd discharging capacities of each group.

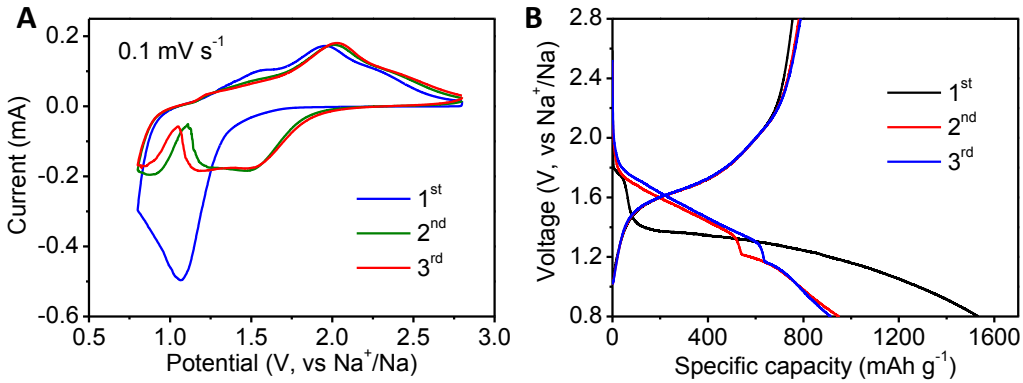

fig. S12. CV curves and voltage profiles of pPAN/SeS_2 for Na storage. (**A**) CV curves at 0.1 mV s^{-1} and (**B**) voltage profiles at 0.1 A g^{-1} of the RT Na-SeS_2 battery in the voltage range of 0.8 – 2.8 V *vs* Na^+/Na.

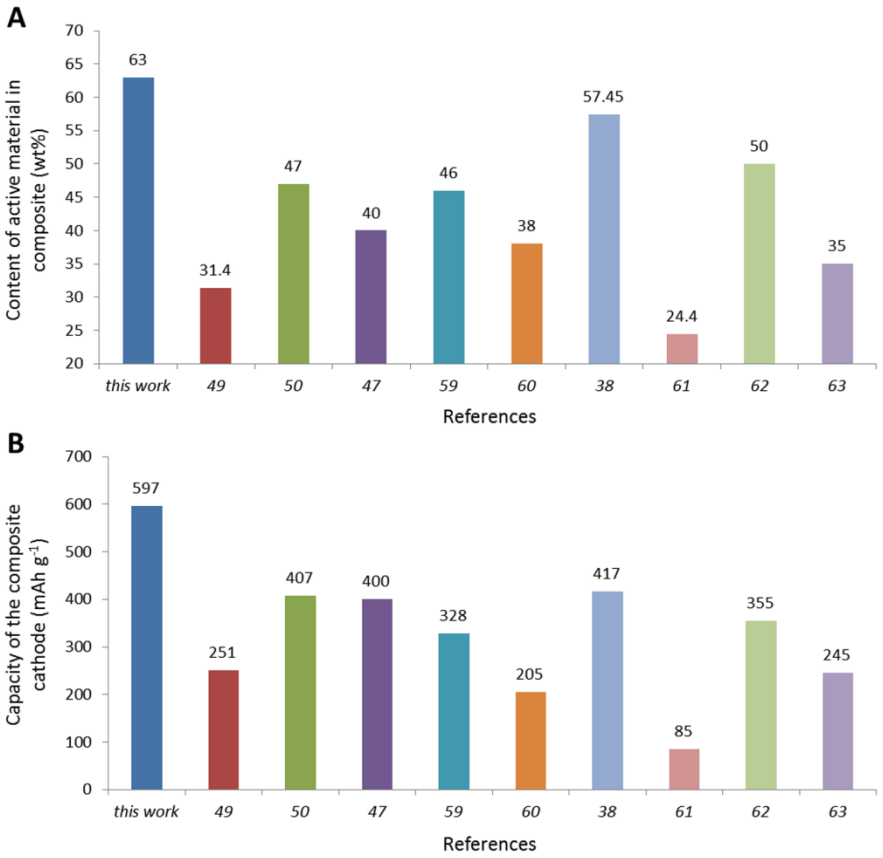

fig. S13. Comparisons of RT Na-S and Na-Se/S batteries. Comparisons of (**A**) active material contents in the composites and (**B**) overall capacities of the composites. Since the 1st discharge capacities are usually accompanied with side reactions, the capacity values are based on the 2nd discharge capacities of the composites. The composite cathodes for comparison are selected from recent studies of RT Na-S batteries: c-PANS(*49*), MCPS1(*50*), S/(CNT@MPC)(*47*), S@iMCHS(*59*), C/S(*60*), $S_{0.6}Se_{0.4}$@CNFs(*38*), CFC/S(*61*), HSMC-Gu-S(*62*), and C/S(*63*).